Catalysis Today 158 (2010) 409–414

Contents lists available at ScienceDirect

Catalysis Today

journal homepage: www.elsevier.com/locate/cattod

Effect of Si/Al ratio of the starting NaY on hydro-upgrading catalyst performance

Fucun Wang[a,b], Liang Wang[c], Jinling Zhu[b], Xuejun Zhang[b], Zifeng Yan[a,**], Fang Fang[c], Ran Tian[b], Zhihua Zhang[b], Baojian Shen[c,*]

[a] State Key Laboratory of Heavy Oil Processing, CNPC Key Laboratory of Catalysis, China University of Petroleum, Qingdao 266555, China
[b] Daqing Petrochemical Research Center of PetroChina, Daqing 163714, China
[c] State Key Laboratory of Heavy Oil Processing, CNPC Key Laboratory of Catalysis, China University of Petroleum, Beijing 102249, China

ARTICLE INFO

Article history:
Available online 13 July 2010

Keywords:
Si/Al ratio
NaY
Type II phase
Hydro-upgrading catalyst

ABSTRACT

The effect of Si/Al ratio of the starting NaY on hydro-upgrading catalyst performance for LCO was studied. Y type zeolite modified from higher Si/Al ratio of the starting NaY also had higher framework Si/Al ratio. Three catalysts of W-Ni supported on different modified Y type zeolites and Al_2O_3 were prepared by impregnation method. The catalysts were characterized by XRD, BET, DRS and HRTEM, and evaluated with a micro-reactor using tetralin as a model compound and a 100 ml hydrogenation test unit using FCC LCO as feedstocks. By contrast, tungsten supported on Y type zeolite modified from higher Si/Al ratio of the starting NaY zeolite had more type II active phase and WS_2 is highly stacked, exhibiting the weak interaction with Al_2O_3 and should have higher activity. The revaluation results revealed that the catalyst prepared by higher Si/Al ratio of the starting NaY zeolite has higher tetralin conversion and better hydro-upgrading performance for FCC LCO.

1. Introduction

With the growing demand for diesel fuel, the proportion of the Fluid Catalytic Cracking (FCC) in the diesel pool increases greatly. However, high aromatics content in FCC LCO (Light Cycle Oil) lowers diesel fuel quality, especially cetane number, and brings about the formation of undesirable emissions in exhaust gases from diesel engines. As a result of the gradual change to more stringent environmental regulations, much attention has been paid to the deep reduction of aromatics in diesel distillate. Under such circumstances, there is considerable interest in the development of new catalysts for aromatic hydrogenation [1–3]. Extensive studies have revealed that the addition of acidic components into the traditional alumina-supported hydrotreating catalysts can greatly enhance their hydrodearomatization (HDA) activities [4,5]. The intrinsic activity of the catalysts can be enhanced by supporting the metals on a strongly acidic, high surface area support, e.g., zeolite Beta or Y [6–8]. Supports with varying acidity can influence the activity for dealkylation or C–C bond scission [9]. Among the acidic components, Y type zeolite is the most studied and widely commercially applied [10–12]. In addition, as the bifunctional catalyst, the dispersion of hydrogenation metal active phases is crucial to HDA catalyst activity. The CoMoS(NiWS) model, in which Co(Ni) decorates the edge sites of highly dispersed MoS_2 (WS_2) crystallites, has been accepted as the catalytically active phase in Co-Mo(Ni-W) sulfide catalysts [13–15]. Based on their catalytic activities, there are two types of the CoMoS(NiWS) phase, namely CoMoS(NiWS) Type I and CoMoS(NiWS) Type II. It is suggested that the CoMoS(NiWS) Type I is related to highly dispersed single slab MoS_2(WS_2) particles maintaining their interactions with the support, e.g., Mo–O–Al bonds, while CoMoS(NiWS) Type II is related to less dispersed MoS_2 particles mainly stacked and not linked with the support, the latter showing a higher intrinsic activity for HYD than the former. Consequently, in order to increase catalyst activities, we need to control the interactions between the support surface and active phases to obtain enhanced stackings of MoS_2(WS_2) particles keeping their dispersion high.

The goal of our research is to improve the qualities of the cracked diesel components (LCO), mainly to decrease the number of aromatics and increase the cetane index for a premium diesel fuel production using different Y type zeolites as cracking component for hydro-upgrading catalysts. Comparisons between hydro-upgrading catalysts using Y type zeolite acidic component modified from different Si/Al ratio starting NaY are not well-documented. Vradman et al. concluded that silica supported WS_2 [16] displayed higher stacking number and dearomatization performance compared with γ-Al_2O_3 supported sulfides, so different Si/Al ratio of Y type zeolites may play an important role in dispersion of active phases and catalytic activity of hydro-upgrading catalyst. In this study, we examined the effect of Si/Al ratio of the starting NaY on the catalytic activity of hydro-upgrading catalyst performance.

---

[*] Corresponding author. Tel.: +86 10 89733369; fax: +86 10 89733369.
[**] Corresponding author. Tel.: +86 532 86981856.
E-mail addresses: zfyancat@upc.edu.cn (Z. Yan), baojian@cup.edu.cn (B. Shen).

0920-5861/$ – see front matter © 2010 Elsevier B.V. All rights reserved.
doi:10.1016/j.cattod.2010.05.041

2. Experimental

2.1. Different Si/Al ratio NaY modification

Three USY samples, USY1, USY2 and USY3 were obtained with starting NaY1, NaY2 and NaY3 zeolites of Si/Al ratios 3.8, 4.5 and 5.5 respectively by the same modified methods. The modified procedures are as follows: USY1, USY2 and USY3 were prepared by NH_4^+ exchange of NaY1, NaY2 and NaY3 using a 2.0N aqueous solution of NH_4Cl at 80 °C for 2 h under agitation, followed by washing until absence of Cl^-, drying at 100 °C overnight. Then samples were submitted to a steaming treatment at 600 °C for 6 h. Finally, the samples were calcined in the dry air at 550 °C for 3 h.

2.2. Catalyst preparation

Three Ni-W type catalysts, CAT-1, CAT-2 and CAT-3 were prepared with the same metal loadings of WO_3 and NiO. CAT-1, CAT-2 and CAT-3 were prepared by pore volume co-impregnation the extrudates of USY1, USY2 and USY3 separately and γ-alumina carrier even mixture with an aqueous solution of nickel nitrate hexahydrate and ammonium metatungstate, followed by drying at 393 K for 4 h and calcinating at 783K for 4 h. All the catalysts have a fixed amount of each component, namely, the contents of Y type zeolite and Al_2O_3 were 21 wt% and 51 wt% respectively.

2.3. Characterization

2.3.1. X-ray diffractometer (XRD)

NiO, WO_3, CAT-1, CAT-2 and CAT-3 catalysts were characterized using Rigaku D/max-2500/pc X-ray diffractometer and Cu Kα radiation, voltage of 40 kV, electrical current of 200 mA. The data were recorded with 0.02° step size, 2 s at every step.

The relative crystallinity and unit cell parameters of zeolites were calculated from XRD patterns that were recorded with a SIMADU XRD6000 diffractometer and Cu Kα radiation (0.1542 nm, 40 kV and 40 mA). The zeolite powder was packed in the cavity of a XRD sample holder made of glass. Then the holder was kept in a closed vessel containing a saturated $CaCl_2{\cdot}6H_2O$ solution for 16 h to make the moisture in the sample at constant. The relative crystallinity was estimated by comparing the peak intensities of the modified sample with standard NaY sample. The total intensities of the eight peaks assigned to (3 1 1), (5 1 1, 3 3 3), (4 4 0), (5 3 3), (6 4 2), (8 2 2, 6 6 0), (5 5 5, 7 5 1) and (6 6 4) reflections were used for the comparison according to the following equation:

$$X_{\mathrm{i}} = X_{\mathrm{R}}\left(\frac{\Sigma A_{\mathrm{i}}}{\Sigma A_{\mathrm{R}}}\right)$$

X_{R}: the crystallinity of the standard NaY provided by Lanzhou catalyst company of Petrochina; $\sum A_{\mathrm{i}}$: the sum of eight peaks area of Y type zeolites to be determined; $\sum A_{\mathrm{R}}$: the sum of eight peaks area of standard NaY sample.

The unit cell parameters were calculated from the (5 5 5) reflection peak position that were determined using reflection peak of the silicon powder ($2\theta = 28.443°$) as an internal standard. The framework Si/Al ratio was obtained from the calculated unit cell parameters by using Breck–Flanigen equation [17].

2.3.2. BET (N_2 physisorption)

Nitrogen adsorption/desorption measurements were performed on an Tristar 3000 type surface area and pore structures instrument of American Mike Instrument Company. Before adsorption, the samples were calcined at 823 K for 4 h. Powder samples of 30–40 mg were degassed in a sample preparation station under 473 K and a vacuum of 1.33×10^{-3} Pa for 15 h, then switched to the analysis station for adsorption and desorption at 77 K in liquid nitrogen. Surface area was calculated with the multipoint BET equation with linear region in the P/P_0 range of 0.05–0.35. Pore volume was calculated from the maximum adsorption amount of nitrogen at $P/P_0 = 0.99$.

2.3.3. Diffuse reflectance spectra (DRS)

Diffuse reflectance spectra of three catalysts were recorded using corresponding support as reference on a Hitachi U-4100 Spectrophotometer.

2.3.4. High-resolution transmission electron microscopy (HRTEM)

High-resolution transmission electron microscopy (HRTEM) images of the sulfided catalysts were obtained on a Philips Tecnai G2 F20 transmission electron microscope operated at an accelerating voltage of 200 kV. The catalysts were sulfided with a 10 vol.% CS_2/cyclohexane mixture at 330 °C and 4 MPa for 4 h and kept in cyclohexane before measurement. For WS_2 on the catalysts, the average number of layers per slab and average length of slabs were calculated from the measurement of about 200 crystallites with the following equations.

$$\text{Average slab length } \bar{L} = \frac{\sum_{i=1}^{n} n_i l_i}{\sum_{i=1}^{n} n_i} \text{ and average number of layers } \bar{N} = \frac{\sum_{i=1}^{n} n_i N_i}{\sum_{i=1}^{n} n_i}$$

where l_{i} is the length of the slab, n_{i} is the number of the particles with the l_{i} length or N_{i} layers, and N_{i} is the number of layers in the particle i. On the basis of 4–5 TEM images taken at different areas of one sample, the WS_2 slab length was measured manually and the average length of the WS_2 slab was calculated.

2.4. Catalytic activity evaluation

2.4.1. Hydrogenation of tetralin

Since monoaromatics are predominant among the possible aromatic compounds in the FCC LCO, tetralin has been used as a probe molecule which is able to diffuse into the supercages of zeolite Y [18,19]. So tetralin was chosen as the model compound for hydro-upgrading catalysts activity evaluation. The catalytic experiments were performed on a micro-reactor. The system consisted of liquid and gas feeding sections, a high-pressure reactor, a heater with a temperature controller for precisely controlling the temperature of the catalyst bed and a high-pressure gas–liquid separator. The reaction was carried out at temperatures of 320 °C and 360 °C in H_2 at a total pressure of 4.0 MPa. Before each catalytic run, the catalyst was sulfided with 10 vol.% CS_2 dissolved in n-decane and at 340 °C for 4 h. The reactor was then brought to the reaction temperature and pressurized to 4 MPa. The liquid hourly space velocity (LHSV) and H_2 to hydrocarbon ratio were maintained at 1.8 h^{-1} and 400, respectively. The reaction time was 7 h. The tetralin feed was diluted with n-decane at a weight ratio of 10:90. The liquid products were collected and were identified by using GC–MS and quantified by a Varian 3400 GC. The GC was equipped with a DM-5 capillary column (30 m × 0.25 mm × 0.32 μm). The HDA activity of tetralin was calculated as follows:

$$\text{Tetralin conversion } (\%) = \left[\frac{(T_{\text{feed}} - T_{\text{product}})}{T_{\text{feed}}}\right] \times 100$$

where T_{feed} and T_{product} denote the tetralin content in the feed and product.

2.4.2. Hydrogenation of FCC LCO

In contrast with FCC LCO, tetralin is free of sulfur and nitrogen impurities, sulfur and nitrogen compounds are considered to be poisons for metal catalysts and can influence the activity of

Table 1
Si/Al ratio and relative crystallinity of NaY and USY.

Samples	Framework Si/Al ratio	Relative crystallinity[a] (%)
NaY1	3.8	95
NaY2	4.5	94
NaY3	5.5	96
USY1	22.3	74
USY2	26.5	81
USY3	31.4	90

[a] The NaY zeolite sample was provided by Lanzhou company of Petrochina, which had a defined crystallinity, and was used as the standard for crystallinity comparison.

hydrotreating catalysts. The evaluation results for tetralin may not be persuasive, therefore hydro-upgrading of Daqing FCC LCO (aromatics content: 56.9 vol.%) over CAT-1 CAT-2 and CAT-3 was also conducted on 100 ml continuous flow fixed-bed hydrogenation test units and single-stage, one catalyst, once-through process was adopted. The total aromatic contents of the feedstocks and diesel products were determined by the standard method of fluorescence indicator adsorption (FIA). The catalysts were sulfided in situ before evaluation, sulfidation oil was a kind of straight kerosene containing 2 wt% CS_2. HDA activity of three catalysts was expressed in terms of aromatics conversion:

$$\text{Aromatics conversion}\,(\%) = \left[\frac{(A_{\text{feed}} - A_{\text{product}})}{A_{\text{feed}}}\right] \times 100$$

where A_{feed} and A_{product} denote the aromatics content in the feed and product.

3. Results and discussion

3.1. XRD

Framework Si/Al ratio and relative crystallinity of NaY and USY are listed in Table 1.

Table 1 summarizes the results that Si/Al ratios and relative crystallinity of USY increase as starting NaY zeolite Si/Al ratios increase, which indicates hydrothermal stability of USY zeolites is different. The higher zeolite Si/Al ratio, the higher zeolite relative crystallinity, the more stable the structure of the zeolite [20,21], which is in great agreement with the following XRD patterns.

The XRD profiles of the oxidic samples are shown in Fig. 1. The characteristic diffraction peaks of WO_3 ($2\theta = 23.1°$, $23.6°$ and $24.4°$) and NiO ($2\theta = 37.3°$ and $43.4°$) did not appear in CAT-1, CAT-2 and CAT-3. This means that the tungsten and nickel oxidic species were either completely amorphous or composed of crystallites smaller than 4 nm [22,23]. WO_3 and NiO were considered evenly distributed on the surface of the support. The characteristic diffraction peaks of γ-Al_2O_3 ($2\theta = 37.2°$, $45.9°$, and $66.8°$) and Y type zeolite ($2\theta = 12°$, $16°$, $19°$, $20°$ and $24°$) appeared in all samples. Three catalysts have the same peak position. CAT-2 and CAT-3 have similar peak intensity, but CAT-1 has lower peak intensity than CAT-2 and CAT-3, this evidence suggests the removal of framework aluminum resulted in a less ordered framework structure and a contraction in the lattice, consistent with the results of Ref. [24], and NaY1 is easily removal of framework aluminum than NaY2 and NaY3, this is in consistent with basic properties mentioned in Table 1 of three Y type zeolites.

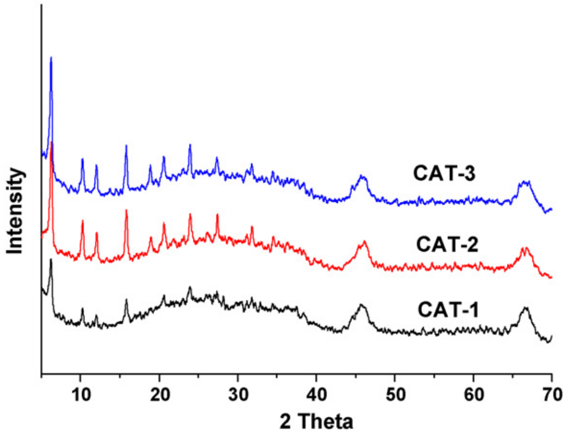

Fig. 1. XRD patterns of CAT-1, CAT-2 and CAT-3.

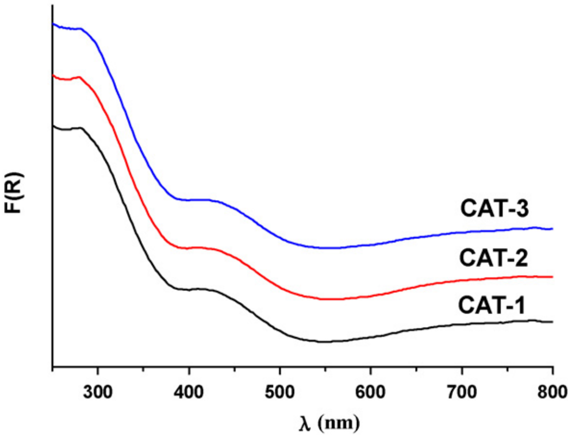

Fig. 2. DRS spectra of (a) CAT-1, CAT-2 and CAT-3.

3.2. Pore structures of USY1, USY2 and USY3

According to N_2 adsorption/desorption analysis of USY1, and USY2 and USY3 in Table 2, mesopore structures of Y type zeolites were produced after modification, which made catalysts be suitable for hydrotreating large molecule feed oil, such as aromatics hydrocarbon. Three USY zeolites had no significant essential differences in their fundamental pore structures, irrespective of the starting NaY zeolites used.

3.3. DRS

In previous literature [25], the authors analyzed Ni^{2+} state on the supports of P-Ni-W/Al_2O_3 catalysts, they thought that bands at 580 nm and at 640 nm in the DRS spectrum of P-Ni-W/Al_2O_3 catalysts were assigned to Ni^{2+} in $NiAl_2O_4$, which is a kind of inactive nickel spinel. The diffuse reflectance spectra of CAT-1, CAT-2 and CAT-3 are presented in Fig. 2., no obvious peaks at 580 nm and 640 nm are found in the spectra of three catalysts ascribed to the

Table 2
Pore structures of USY1, USY2 and USY3.

Zeolites	BET surface area (m^2/g)	Meso pore surface area (m^2/g)	Total volume (ml/g)	Micro pore volume (ml/g)
USY1	613	124	0.33	0.24
USY2	630	119	0.36	0.25
USY3	622	121	0.34	0.22

presence of tetrahedrally coordinated Ni^{2+} ions in a spinel-type $NiAl_2O_4$ in the spectra of NiW/Al_2O_3. But it can be clearly seen that the band around 420 nm, characteristic of octahedrally coordinated Ni^{2+} ions, revealing an enhanced incorporation of nickel with tungsten producing Ni-W-O species [26]. Additionally, it can be concluded that the Ni^{2+} ions are liable to be octahedrally coordinated on the composite support USY/Al_2O_3, due to the modifying effects of USY on alumina, which impedes inactive nickel spinel formation effectively, facilitating the promotion effect of nickel on tungsten. The curves of three catalysts are almost identical, so the promotion effect of nickel had no big difference on three catalysts.

3.4. HRTEM

The representative HRTEM micrographs of the three sulfided catalysts are given in Fig. 3. The slab length (Fig. 4A) and layer number (Fig. 4B) distributions are illustrated in Fig. 4. It can be seen that CAT-3 significantly increases the fraction of the WS_2 slabs larger than 7 nm compared with CAT-1 and CAT-2, with the average length of the WS_2 slabs increasing from 4.84 nm for catalyst CAT-1 and 5.09 nm for CAT-2 to 5.71 nm for catalyst CAT-3. This indicates that the dispersion of the active phase WS_2 is greater on catalyst CAT-3 than on catalyst CAT-1 and CAT-2. As shown in Fig. 3., the WS_2 slabs on CAT-3 are more stacked than those on CAT-2 and CAT-1, because weaker support-O-WS_2 bonds can be more easily cleaved, and thus highly stacked WS_2 particles are formed [27], the highly stacked WS_2 slabs on CAT-3 are attributed to the weaker metal-support interaction. Extensive research [28–30] has shown that there are at least two types of “Ni-W-S” phases in alumina-supported NiW sulfided catalysts. The type I phase is less stacked, containing some W-O-Al linkages with the alumina support related to the strong interaction between W and hydroxyl groups on the alumina surface and thus having lower activity. The type II phase is highly stacked, exhibiting the weak interaction with alumina and thus showing higher activity. Multilayered WS_2 slabs provided a higher density of multivacancies compared with single-layered or thin slabs. This could facilitate π-complexation of the aromatic ring on multilayered WS_2 slabs relative to single-layered or thin slabs [31]. Therefore, hydrogenation activity of the catalyst was greatly improved. The HRTEM characterization results of the corresponding sulfided catalysts suggested that the activities of three catalysts are as follows: CAT-3 > CAT-2 > CAT-1. It has been demonstrated that the size of WS_2 is mostly related to the distribution of WS_2 on the surface of Al_2O_3 [32]. Compared with CAT-2 and CAT-3, the smaller size of WS_2 on CAT-1 was produced because of more Al_2O_3 available to distribute on. Taking the support as a whole, the quantity of surface Al_2O_3 of CAT-3 is less than CAT-1 and CAT-2. Consequently, larger WS_2 was formed on the surface of CAT-3 than that of CAT-1 and CAT-2. Therefore, different Y type zeolite supports resulted in different activities of three catalysts. The higher framework Si/Al ratio of Y type zeolite resulted in a higher proportion of Si distribution on the surface of NiW/Y. The more silica the surface has, the longer and more layer number of WS_2 slabs are formed.

3.5. Comparison of hydro-upgrading performance for tetralin

Tetralin conversion for three catalysts is shown in Fig. 5. Fig. 5 displays that the crucial factor for hydro-upgrading performance is not the reaction temperature, but hydro-upgrading catalysts. CAT-3 has the highest tetralin conversion and CAT-1 has the lowest tetralin conversion among three catalysts both at 320 °C and 360 °C, it is generally accepted that the high-silica samples exhibited higher cracking rates, the rate increased with the increasement of Si/Al ratio [20]. Based on the aforementioned results, it can be concluded that the higher conversion of zeolite-containing catalyst was associated primarily with different Y type zeolites, the catalyst made by Y type zeolites modified from the higher starting NaY Si/Al ratio had higher stacking number of WS_2 phase, which can enhance hydro-upgrading catalyst activity.

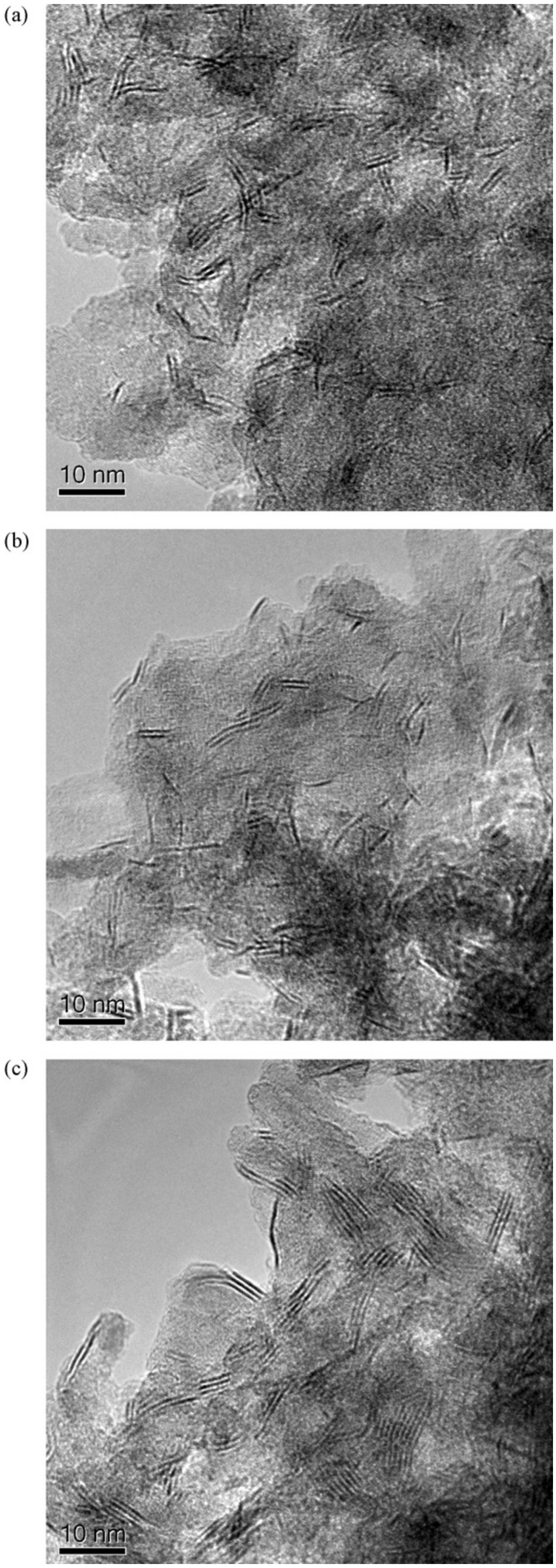

Fig. 3. HRTEM micrographs of sulfided catalysts (a) CAT-1, (b) CAT-2, (c) CAT-3.

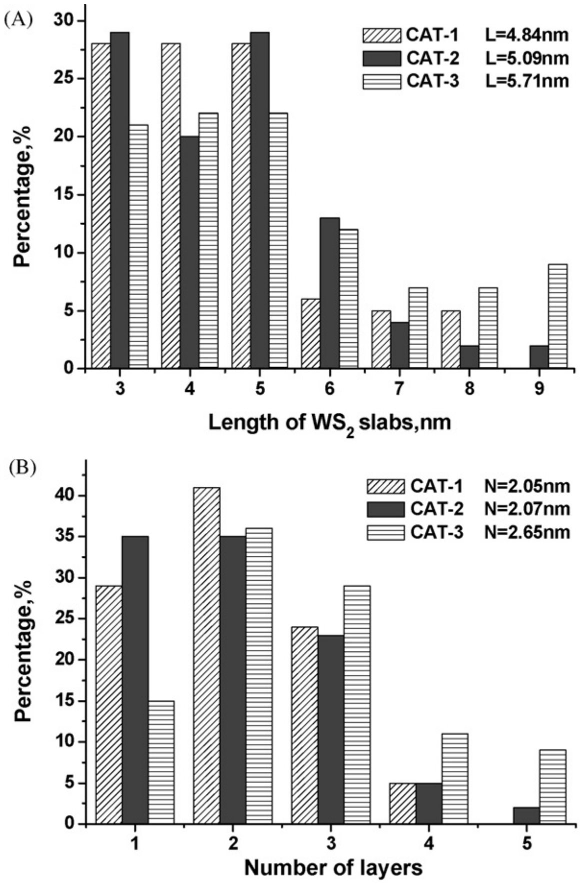

Fig. 4. Crystal size distribution of WS_2 for sulfided catalysts: slab length (A), number of layers (B).

3.6. *Comparison of three catalysts hydro-upgrading performance for FCC LCO*

The comparison of dearomatization performance of CAT-1, CAT-2 and CAT-3 in dearomatization of FCC LCO at selected conditions is depicted in Fig. 6.

The evaluation results exhibited that CAT-3 catalyst showed better HDA performance than that of CAT-1 and CAT-2 at different reaction pressure. The results demonstrated that higher HDA activity of CAT-3 catalyst was associated primarily with relatively higher WS_2 slabs, which was inherited from the different Y type zeolite supports. Thus Y type zeolite support modified from higher Si/Al ratio of the starting NaY is more suitable for preparation of dearomatization catalysts compared with Y type zeolite support modified from lower Si/Al ratio of the starting NaY. The evaluation results revealed that there was parallel catalytic performance of three catalysts in hydrogenation of model compound and dearomatization of petroleum feedstocks.

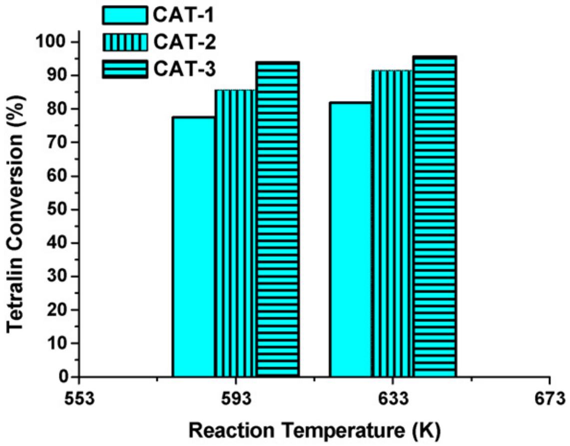

Fig. 5. Tetralin conversion of CAT-1, CAT-2 and CAT-3 at 320 °C and 360 °C, respectively.

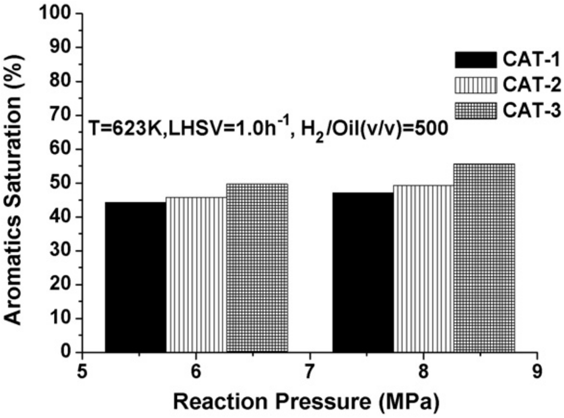

Fig. 6. Comparison of the HDA performance of CAT-1, CAT-2 and CAT-3.

4. Conclusions

In the present study it was found that Si/Al ratio of the starting NaY zeolite had an important influence on the performance of modified Y type zeolites and catalysts. Y type zeolites modified from higher Si/Al ratio of the starting NaY also had higher framework Si/Al ratio. W-Ni catalysts supported on different modified Y type zeolites and Al_2O_3 were prepared by wetness impregnation method. XRD results showed that relative crystallinity of modified Y type zeolite increased as the starting NaY Si/Al ratio increased, a higher Si/Al ratio resulted in better hydrothermal stability of Y type zeolite. N_2 adsorption/desorption analysis of three USY zeolites demonstrated that three zeolites had no significant essential differences in their fundamental pore structures, irrespective of the strating NaY zeolites used. The DRS curves of three catalysts were identical, therefore the promotion effect of nickel had no big difference for three catalysts. HRTEM results revealed that tungsten supported on Y type zeolite modified from higher Si/Al ratio of the starting NaY zeolite had more type II active phase and WS_2 is highly stacked, exhibiting the weak interaction with alumina and should have higher activity. The revaluation results revealed that the catalyst prepared by higher Si/Al ratio of the starting NaY zeolite had higher tetralin conversion and better hydro-upgrading performance for FCC LCO.

Acknowledgment

The authors gratefully acknowledge the funding of the research project under contract number 06-03A-01-05 by PetroChina for financial support.

References

[1] C. Song, Catal. Today 86 (2003) 211.
[2] L. Huang, Q.L. Huang, H.N. Xiao, M. Eic, Micropor. Mesopor. Mater. 111 (2008) 404.
[3] Takashi Fujikawa, Kazuo Idei, Takeshi Ebihara, Hirofumi Mizuguchi, Kazushi Usui, Appl. Catal. A 192 (2000) 253.
[4] E. Lecrenay, K. Sakanishi, I. Mochida, Catal. Today 39 (1997) 13–20.
[5] I. Isoda, S. Nagao, X. Ma, Y. Korai, I. Mochida, Energy Fuels 10 (1996) 1078.

[6] N. Matsubayashi, H. Yasuda, M. Immamura, Y. Yoshimura, Catal. Today 45 (1998) 375.
[7] C.C. Costa Augusto, J.L. Zotin, A. da Costa Faro, Catal. Lett. 75 (2001) 37.
[8] B. Pawelec, R. Mariscal, R.M. Navarro, S.V. Bokhorst, S. Rojas, J.L.G. Fierro, Appl. Catal. A 225 (2002) 223.
[9] W.R.A.M. Robinson, J.A.R. van Veen, V.H.J. de Beer, R.A. van Santen, Fuel Process. Technol. 61 (1999) 104.
[10] L.H. Ding, Y. Zheng, Z.S. Zhang, Z. Ring, J.W. Chen, Catal. Today 125 (2007) 229.
[11] F. Bataille, J.L. Lemberton, G. Pérot, P. Leyrit, T. Cseri, N. Marchal, S. Kasztelan, Appl. Catal. A 220 (2001) 191–205.
[12] N. Kunisada, K. Choi, Y. Korai, I. Mochida, K. Nakano, Appl. Catal. A 276 (2004) 51–59.
[13] B.S. Clausen, S. Mørup, H. Topsøe, R. Candia, J. Phys. C 37 (1976) 249.
[14] H. Topsøe, R. Candia, N.-Y. Topsøe, B.S. Clausen, Bull. Soc. Chim. Belg. 93 (1984) 783.
[15] H. Topsøe, B.S. Clausen, N.-Y. Topsøe, E. Pedersen, Ind. Eng. Chem. Fundam. 25 (1986) 25.
[16] L. Vradman, M.V. Landau, M. Herskowitz, Fuel 82 (2003) 636.
[17] D.W. Breck, E.M. Flanigen, Molecular Sieves, Soc. Chem. Ind., Lond. (1968) 47.
[18] M. Santikunaporn, J.E. Herrera, S. Jongpatiwut, D.E. Resasco, W.E. Alvarez, E.L. Sughrue, J. Catal. 228 (2004) 100.
[19] H.R. Liu, X.C. Meng, D.S. Zhao, Y.D. Li, Chem. Eng. J. 140 (2008) 425.
[20] Bin Xu, Silvia Bordiga, Roel Prins, A. Jeroen, van, Bokhoven, Appl. Catal. A 333 (2007) 245–253.
[21] A. Abraham, S.H. Lee, C.H. Shin, S.B. Hong, R. Prins, J.A. van Bokho-ven, Phys. Chem. Chem. Phys. 6 (2004) 3031.
[22] L.H. Ding, Y. Zheng, Z.S. Zhang, Z. Ring, J.W. Chen, J. Catal. 241 (2006) 438.
[23] L.H. Ding, Y. Zheng, Z.S. Zhang, Z. Ring, J.W. Chen, Appl. Catal. A 319 (2007) 26.
[24] H.F. Li, M.F. Li, Y. Chu, H. Nie, Micropor. Mesopor. Mater. 117 (2009) 636.
[25] P. Atanasova, T. Halachev, Appl. Catal. A 108 (1994) 123.
[26] B.J. Shen, H.F. Li, W.C. Zhang, Y. Zhao, Z.H. Zhang, X.H. Wang, S.K. Shen, Appl. Catal. A 106 (2005) 208.
[27] Usman, T. Kubota, Y. Araki, K. Ishida, Y. Okamoto, J. Catal. 227 (2004) 523.
[28] H. Topsøe, B.S. Clausen, Catal. Rev. Sci. Eng. 26 (1984) 395.
[29] H. Topsøe, B. Hinnemann, J.K. Nørskov, J.V. Lauritsen, F. Besenbacher, P.L. Hansen, G. Hytoft, R.G. Egeberg, K.G. Knudsen, Catal. Today 107–108 (2005) 12.
[30] B. Hinnemann, J.K. Nørskov, H. Topsøe, J. Phys. Chem. B 109 (2005) 2245.
[31] L. Vradman, M.V. Landau, Catal. Lett. 77 (2001) 53–54.
[32] Y.W. Li, X.Y. Pang, B. Delmon, J. Mol. Catal. A: Chem. 169 (2001) 259.